Performance Analysis of a Full-Duplex TWDM-PON Using OFDM Modulation with Red LED Visible Light Communication System

Meet Kumari[1] · Anu Sheetal[2] · Reecha Sharma[1]

Abstract

Today's access networks are in high demand to fulfill the high bandwidth requirement because of extensive improvement in high transmission rate applications for cloud computing, big data analytics, and other next-generation 5G smart applications. In this work, the symmetrical and bidirectional time and wavelength division multiplexing-passive optical network (TWDM-PON) system is proposed and demonstrated. Orthogonal frequency division multiplexing (OFDM) with 4-level quadrature amplitude modulation is used for downstream and upstream transmission. Also, 625 nm red light-emitting diode is utilized for visible light communication (VLC) using a wireless link to encourage the economic high transmission rate fiber/VLC optical network. The TWDM-PON employing OFDM with the VLC system has been analysed for downstream and upstream channels for variable fiber-wireless link range. Additionally, the impact of a high transmission rate and usage of digital signal processing (DSP) unit to reduce losses due to fiber nonlinearity effects in the proposed link has been investigated. The results show that the maximum faithful wireless and wired range for the proposed system is 140 m and 60 km respectively at 20 Gbps to attain the minimum 3.8×10^{-3} BER. The decrease in error vector magnitude (EVM%) by almost 52% with the use of DSP in the proposed system provides a high transmission rate of 200 Gbps in the proposed link. Further, comparative performance of the proposed system with previous latest works in literature reveals a superior performance of the proposed link. The proposed TWDM-PON system provides a next-generation access network from rural areas to urban areas.

Keywords DSP · NG-PON · OFDM · PON · TWDM · VLC

✉ Meet Kumari
meetkumari08@yahoo.in

1   Department of Electronics and Communication Engineering, Punjabi University, Patiala, Punjab, India

2   Department of Electronics and Communication Engineering, Guru Nanak Dev University Regional Campus, Gurdaspur, Punjab, India

1 Introduction

Recently, the requirements of high-capacity access networks are growing exponentially because of the rise in popularity of big-data analytics, cloud computing and ultra-high-resolution video broadcast. To provide broadband capacity and cost-effective last-mile network to all end-users, the emerging passive optical network (PON) and the optical wireless system would be the favorable systems for high-speed data transmission [1–3]. Further, the primary point-to-multipoint (P2MP) PON architectures comprise the usage of time-division-multiplexing (TDM) or wavelength-division-multiplexing (WDM) techniques [4–6]. Thus, for high capacity PON systems as well as to meet the end users' high bandwidth demands, a next-generation passive optical network (NG-PON) based bidirectional 40 Gbps time- and wavelength-division-multiplexing passive optical network (TWDM-PON) access network has been proposed and successfully demonstrated.

Further, to acquire 100 Gbps with TWDM design, various solutions for the upstream and downstream modulation format, like on–off keying (OOK), 4-level pulse amplitude modulation (4-PAM), and duobinary has been proposed and investigated [7]. Lin et al. [8] proposed and demonstrate an asymmetric 100/40 Gbps (downstream/upstream) TWDM-PON with downstream double side-band orthogonal frequency-division multiplexing (DSB OFDM) modulation and upstream OOK modulation signals over a 20 km optical fiber. Šprem and Babić [9] proposed and demonstrated the symmetric 55 Gbps wavelength division multiplexing PON (WDM-PON) with OOK modulation for downstream and upstream signals with channel spacing of 100 GHz and 50 GHz at 30 km fiber distance. Tang et al. [10] proposed and investigated the symmetric 40 Gbps 4-PAM PON with low-complexity equalizers for 20 km fiber distance. Zhang et al. [11] proposed and demonstrate the symmetric 10 Gbps WDM-PON with differential quadrature phase-shift keying (DQPSK) and OOK modulation for downstream and upstream signals at 20 km distance. Shao et al. [12] proposed and simulated symmetric 10 Gbps PON employing 4-PAM modulation at 20 km distance. Thus, for the 40–100 Gbps PON access using 4-PAM, OOK and duobinary on single wavelength in standard 20 km PON reach are not much more realizable because of the optical fiber constraints such as polarization mode dispersion, chromatic dispersion (CD) and pricey 40 GHz transceivers [7, 13]. For the future 40–100 Gbps PON, to achieve a higher data rate economically, the high spectrum efficiency quadrature amplitude modulation orthogonal frequency division multiplexing (QAM-OFDM) modulation would be used [14].

Recently, a 100 Gbps downstream and 40 Gbps upstream asymmetric TWDM-PON has been analyzed by utilizing broadband QAM-OFDM signal. Although they required a re-modulation scheme at optical network unit (ONU) for upstream channels using an electro-absorption modulator (EAM) and higher-order of sampling rate for OFDM processing [15]. Also, the OFDM subcarriers would be influenced by the higher frequency owing to the CD and radio frequency (RF) power fading in a fiber network. QAM-OFDM is a spectrally effective modulation format that encodes the information on multiple orthogonal subcarriers. Contrarily, TDM and WDM support time and wavelength multiplexing of distinct channels respectively; hence permitting several consumers to access and share the single transmission link. Apart from TDM and WDM, OFDM can allow dynamic bandwidth allocation, a better degree of freedom, and software reconfigurable [16–18]. However, the TWDM-PON using QAM-OFDM modulation, a fiber access network may not be an adequate choice in certain areas where the fiber installations are costly because of the geographical restrictions [19–21]. Here,

the most favorable, visible light communication (VLC) technology can be effectively utilized and combined with the PON to fix this issue [22–24]. A light-emitting diode (LED) enabled the VLC system has many benefits such as the high data rate, protocol transparency, high security, license-free spectrum range (384–789 THz), infrastructure flexibility, full-duplex and economical transmission link [13, 25, 26]. Besides this, the VLC also can provide electromagnetic interference (EMI)-free optical free space access in both indoor and outdoor environments. Additionally, the VLC systems are installed and used for the backup fiber, point-to-point last-mile access and organization connectivity to support system security and geographical constraints [27–29]. Therefore, the advantages of TWDM PON- using QAM-OFDM modulation with the VLC system have attracted many researchers' attention. Chen et al. [30] reports the effective transmission of 157.5 Mbps information in 2×2 multiple inputs–multiple-output (MIMO)–OFDM VLC system over the VLC link range of 0.5 m. In another work by Li et al. [31] report the faithful transmission of 682 Mbps information in the VLC system using OFDM modulation over the 1 m VLC link. Also, the effective transmission of 519.8 Mbps information in the QAM OFDM-VLC system combined with the multi-band constant amplitude zero autocorrelation sequence (MB-CAZAC) over VLC link distance of 50 cm for different modulation schemes is reported [32]. Lu et al. [33] and Deng et al. [34], report the successful transmission of 30 Mbps and 3.63 Gbps data respectively in hybrid OFDM-VLC system over a VLC distance of 3.5 m. Chow et al. [35] reports successful transmission of 6.14 Mbps data over 2 m VLC link range in the VLC system with adaptive control of OFDM. Zhang et al. [36], experimentally demonstrates the reliable transmission of 1.87 Gbps information over a 0.8 m VLC link-based WDM-VLC system utilizing OFDM. Again, the effective transmission of 682 Mbps data in multi-channel uplink VLC system utilizing time division multiple access (TDMA) scheme and OOK modulation over the VLC link range of 6.2 m is reported [37]. Chi and Shi [38] experimentally demonstrate a 2×1.6 Gbps VLC system utilizing OFDM modulation over a VLC link range of 1.1 m.

Although a lot of previous works have demonstrated on VLC-OFDM system, none of the works discusses the performance of TWDM-PON using QAM-OFDM modulation with the VLC system. He et al. [39] reports the successful transmission of 10 Gbps carrierless amplitude phase (CAP) modulation signal in integrated WDM–CAP–PON and visible laser light communication (VLLC) system over a fiber and free-space optics (FSO) link range of 20 km and 4.5 m respectively. Also, Wei et al. [40], presents the transmission of 2.5 Gbps–10 GHz information in the fiber-VLLC system using OFDM over 20 km fiber and 8 m VLLC distance. In another work by Shi et al. [41], demonstrates the faithful transmission of 3.2 Gbps data in OFDM/offset QAM (OFDM/OQAM) based WDM-VLLC system over 50 km fiber and 4.5 m VLLC link. However, these fiber-VLC systems using a laser diode (LD) are applicable for short-reach access networks at a high cost. VLC system with a low-cost and low power LED provides an energy-efficient transmission system.

Thus, in this paper, the symmetrical and full-duplex TWDM-PON using QAM-OFDM modulation with LED enabled VLC system is proposed and analysed. The proposed TWDM-PON system using four pairs of downstream and upstream wavelengths is operated within 15 GHz bandwidth and each OFDM band is modulated at the four-level QAM (4-QAM) format. Here, coherent detection is employed to provide excellent frequency selectivity as well as receiver sensitivity. Meanwhile, the VLC system using LED light can enhance the bit rate and transmission distance. Here, in Sect. 2, the proposed system design is introduced. Section 3 illustrates the results and discussion, followed by the conclusion in Sect. 4.

2 Concept and System Architecture of Bidirectional TWDM-PON Using OFDM Modulation with VLC

Figure 1 presents the conceptual diagram of TWDM-OFDM PON with the VLC system for integrated fiber and optical wireless access system. The transmitted signal coming from the optical line terminal (OLT) goes through an optical fiber and a remote node (RN) is utilized to allocate the signal to the N numbers of ONUs. In all ONUs, wired and wireless services can be obtained by connecting fibers and through the indoor optical wireless channel by utilizing red illumination LEDs in the ceiling [42].

The proposed architecture of the bidirectional 2.5–200 Gbps TWDM-PON using OFDM modulation with VLC is illustrated in Fig. 2. Here, in OLT, four pairs of continuous wave (CW) frequencies ({187.8, 195.6}, {187.7, 195.5}, {187.6, 195.4} and {187.5, 195.3}) in THz having 100 GHz of channel spacing used for downstream (Tx_{DN}) and upstream (Tx_{UP}) transmission in the system.

As shown in Fig. 2, in the downstream transmission, the four downstream frequencies with modulated OFDM signals are multiplexed by the ideal multiplexer (Ideal Mux) and then passed through downstream single-mode fiber (SMF) followed by a bidirectional splitter. After amplification by an optical amplifier, the downstream signals are distributed to ONUs by an ideal de-multiplexer [43]. At the ONUs side, the receiver prefers its definite frequency and later decodes the OFDM signal. Then the VLC signal is generated
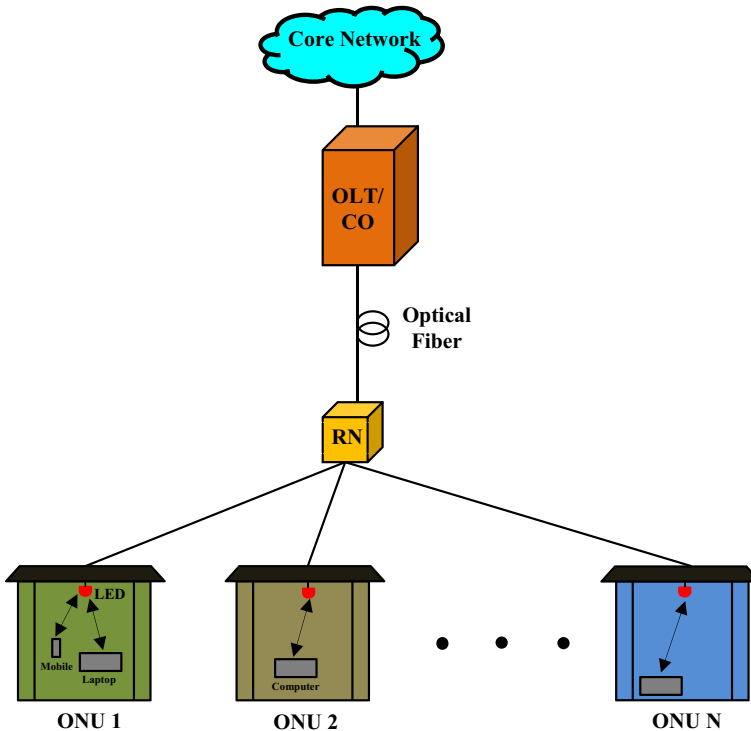

Fig. 1 Conceptual diagram of TWDM-PON system employing OFDM modulation with a red LED VLC system
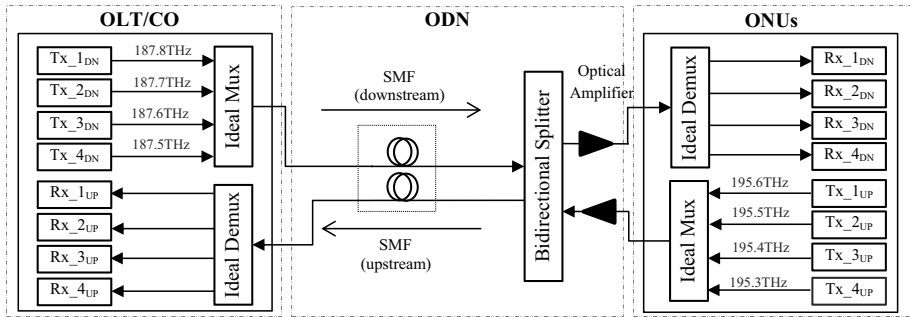
Fig. 2 Schematic of bidirectional 4×2.5 Gbps TWDM-OFDM PON transmitter–receiver with VLC system

by a red LED (480 THz, bandwidth = 1 GHz). A red LED VLC system is a high-quality communication system as the usage of a red LED outperforms other LEDs color combinations [44]. In the upstream transmission, each ONU transmits boosted OFDM signals by an optical amplifier with assigned frequencies transmitted through upstream SMF. At the central office (CO), the upstream signals are de-multiplexed and decoded by an allocated upstream receiver and passed through VLC wireless links. Compared with 16-QAM and 64-QAM, 4-QAM can lessen the requirement of signal to noise ratio (SNR) and provides superior performance in the form of receiver sensitivity [1]. Also, the 4-QAM modulation format tends to transmit 100 Gbps and more information over a single channel but suffer from fiber nonlinearity, phase loss and multipath fading which restrict the maximum successful transmission distance. These restrictions can be diminished by employing coherent detection and DSP unit at the receiver side for improved performance. Thus in this paper, 4-QAM mapping is selected for downstream and upstream transmission in TWDM-OFDM PON with the VLC system [7, 45]. The transmission of 20/3 Gbps (downstream/upstream) information using OFDM-PON signals over 83.7 km SMF link with DSP unit at the receiver side for improved performance has been presented in [6]. Yang et al. [46] discussed the transmission of 10 GS/s TDM-OFDM-PON signals over 26.7 km SMF links with the DSP unit for enhanced system performance.

The schematic for full-duplex TWDM PON system with 4-QAM-OFDM modulation over fiber link and FSO link for wired and wireless transmission respectively is illustrated in Fig. 3. This system is modulated and analysed using OptiSystem 16.0 software. In this work, the global parameters used for system design are the number of samples and symbol rate i.e. 32,768 and 2.5×10^9 symbols per sec respectively. Both CO and ONU have four pairs of transmitters and receivers. The downstream frequencies (187.8–187.5 THz) and the upstream frequencies (195.6–195.3 THz) for the proposed TWDM-PON system strictly follow the ITU-T channel spacing i.e. 100 GHz. These frequencies are emitted by utilizing four pairs of CW lasers with a linewidth of 0.15 MHz and – 6 dBm input power. One downstream transmitter presented in Fig. 3a constitutes a pseudo-random bit sequence (PRBS) generator providing random binary sequences at 2.5–200 Gbps which are fed to 4-QAM sequence generator having 2-bits per symbol. The 4-QAM signal output is modulated using an OFDM modulator having 512 subcarriers, 64 cyclic prefix points and 1024 fast Fourier transform (FFT) points [47, 48]. Then the OFDM modulator generates the in-phase (I) and quadrature (Q) components of the signal for further transmission in the I/Q optical modulator. These I/Q components are filtered by a pair of low pass cosine
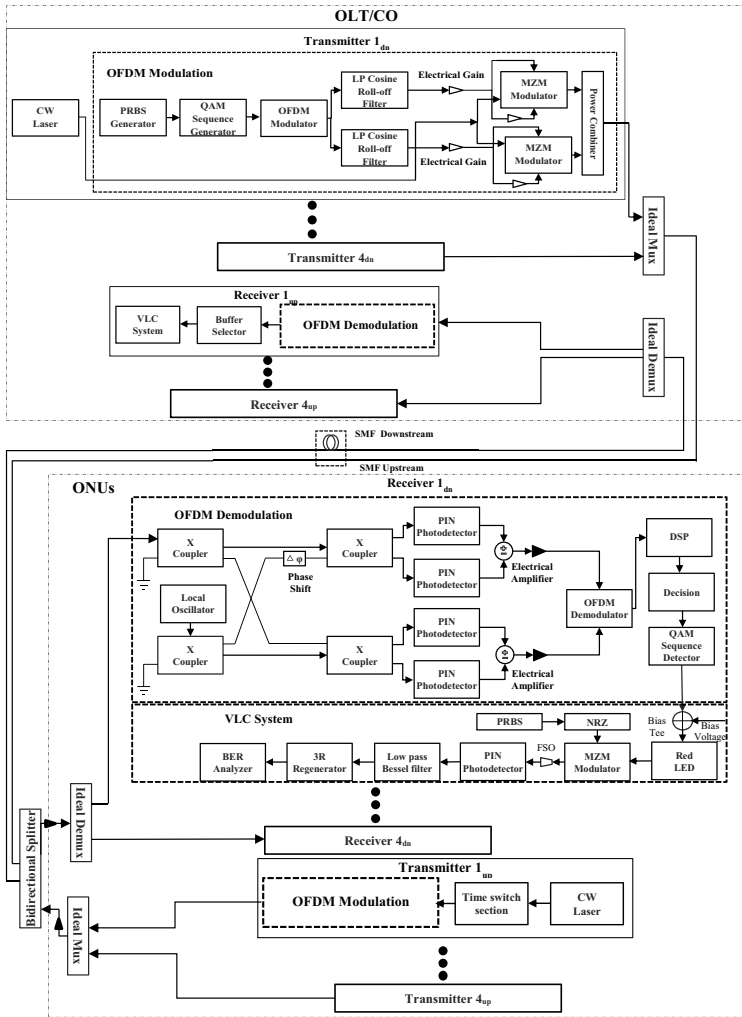
(a)

(b)

Fig. 3 Schematic of **a** full-duplex 4×2.5 Gbps TWDM-PON using 4-QAM OFDM modulation with VLC system and **b** upstream time switch section

roll-off filters having a roll-off factor of 0.2 then send for modulation. Here, the I/Q optical modulator comprises an incoming CW laser signal, two pairs of electrical gain, a pair of mach–Zehnder modulators (MZMs) having a 60 dB extinction ratio, and an optical 2×1 power combiner [20]. Like this, four downstream TWDM-OFDM signals are multiplexed at different frequencies and transmitted over a fiber link where it is distorted because of fiber attenuation, dispersion, and non-linearities effects. After this, the signal is directed to a bidirectional splitter, an optical amplifier with 13 dB gain as well as 4 dB noise figure to enhance the receiver sensitivity of thermal noise (1×10^{-22} W/Hz) limited receiver and transferred to the receiver unit where an opposite operation is accomplished to demodulate the TWDM-OFDM signal. For downstream signal reception, at the ONU side, a single channel de-multiplexed signal is passed to the two pairs of X couplers (coupling coefficient = 0.5) along with a local oscillator and phase shift (phase shift = 90°) components for orthogonal coherent reception. Then, the signal is fed to the two pairs of PIN photodetectors (PD) having responsivity and dark current 1A/W and 10 nA respectively followed by a pair of electrical subtractor, a pair of an electrical amplifier with 20 dB gain and OFDM demodulator. Further, this signal is passed through a DSP module for nonlinearities losses compensation, a decision component and a QAM sequence decoder (bits per symbol = 4 bits) for coherent downstream traffic detection. At the receiver, OFDM demodulator performance parameters should meet with the transmitter to reconstruct the QAM symbols at the output side. The QAM sequence detector identifies the binary sequences and demapped the electrical signal to recover the transmitted bit sequence [15, 21]. Then the DC bias signal (4 V) and electrical signal and are integrated with a bias tee and employed to drive the red LED (625 nm) having a quantum efficiency of 65% in the linear region of operation as shown in Fig. 3a. The incoming LED signal (bandwidth of 1 GHz) is transmitted via the FSO channel after re-modulation by the NRZ-MZM modulator with a 2.5–200 Gbps PRBS signal. Finally, the received data stream is detected at PIN PD and proceeded through a low pass Bessel filter with a cut-off frequency (0.75 × bit rate Hz) followed by a 3R regenerator to recover the received signal. Bit error rate (BER) analyzer is used to analyse the obtained output data stream in terms of quality factor (Q-factor) and BER.

Figure 4 presents the schematic diagram of the single polarization DSP unit. After coherent OFDM demodulation, DSP executes various necessary functions recovering the received signals. It is explained as follows [46]:

1. Bessel filter is utilized with samples per symbol and bandwidth of 8 × samples per bit and 0.75 × symbol rate respectively.
2. Resampling is attained at a rate of four samples per symbol.
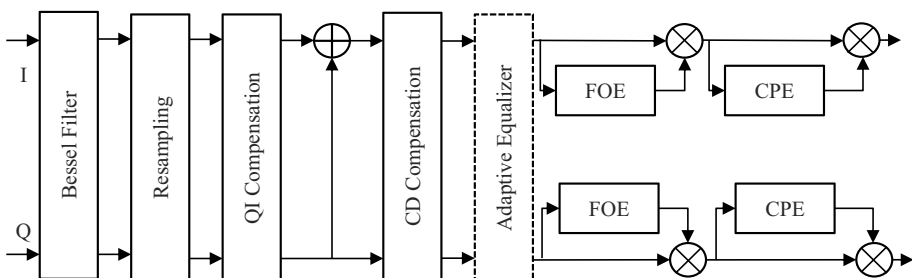

Fig. 4 Single polarization DSP unit

3. Q-imbalance (QI) compensation is used to reduce the phase and amplitude imbalances within I and Q signals respectively.
4. Chromatic dispersion (CD) compensation is used to eliminate CD and fiber nonlinearity through the Back-Propagation algorithm.
5. Adaptive equalizer performs a butterfly structure for de-multiplexing the polarization of the received signal.
6. Frequency offset estimation (FOE) is utilized to eliminate the phase and frequency mismatch between the transmitter and the local oscillator.
7. Carrier phase estimation (CPE) is used to provide better output in terms of transmission distances and bit rates. The signal received at the input of the DSP unit is given as [46]

$$Y(k) = C(k) \cdot e^{j(2\pi \Delta fkT + \varphi_k)} + N(k) \tag{1}$$

where C(k) means the data symbol, Δf, T and φ_k means carrier frequency offset, symbol period and carrier phase respectively, N(k) denotes the zero-mean Gaussian random variable. The received signal in terms of the fourth power can be represented as [46]

$$Y^4(k) = A \cdot e^{4j(2\pi \Delta fkT + \varphi_k)} + E(k) \tag{2}$$

where A and E(k) denote constant amplitude and noise process with zero-mean respectively. Frequency offset can be evaluated by considering the signal's spectral density and it is given as [46]

$$Y^4(k) = \frac{1}{4} arg\big\{ \max \big[|R(f)| \big] \big\} \tag{3}$$

where

$$|R(f)| = \frac{1}{n} \sum_{k=0}^{n-1} Y^4(k) \cdot e^{-j(2\pi \Delta fkT)} \tag{4}$$

where n denotes the block length. A decision component estimates the desired space $|d_{k,b}|^2$ to the nearest constellation point in the 2D complex plane as follows [46]:

$$|d_{k,b}|^2 = \left| R_k e^{-j\varphi_b} - X_{k,b} \right|^2 \tag{5}$$

where $X_{k,b}$ means the decision $R_k e^{-j\varphi_b}$. At last, the received sequences are decoded for the polarization and then parallel to serial converted to obtain the output bits.

Similarly, in the upstream transmission, 4×2.5–200 Gbps OFDM signals are generated with four upstream frequencies. Here, the upstream 2.5–200 Gbps traffic transmitted from the ONUs and detected at the OLT side. The four independent upstream frequencies are transmitted by using four CW lasers with different switching times as shown in Fig. 3b. In the upstream time switch section, each upstream wavelength uses an ideal demux, eight pairs of two cascaded dynamic selects Y to transmit the information at definite timeslot and switching time. The switching time Ts_1 and Ts_2 for two cascaded dynamic selectors 1 and 2 are given respectively as [49]

$$Ts_1 = \text{Timeslot} \cdot \left(\frac{1}{\text{Bit rate}} \right) \cdot \left(\frac{\text{Sequence length}}{T} \right) \tag{6}$$

and

$$Ts_2 = \text{Timeslot} \cdot \left(\frac{1}{\text{Bit rate}} \right) \cdot \left(\frac{\text{Sequence ength}}{T} \right) + \left(\frac{\text{Time window}}{T} \right) \tag{7}$$

where T denotes the number of consumers using the same upstream frequency. Here, T, Timeslot, Sequence length, and Time window values are taken to be 8, 0–7, 8192, and 3.27×10^{-06} s respectively at a reference frequency of 193.4 THz. Table 1 shows the switching time of the proposed system for upstream transmission at 2.5 Gbps.

An ideal mux is used to transfer the upstream switching information for OFDM modulation. After passing the signals from the OFDM modulator and optical amplifier, each upstream wavelength is detected at the CO side using the OFDM demodulator. Also, a buffer selector is used to choose the latest iteration of the simulation. At last, the received signal is directed towards the DSP unit and decision components followed by a VLC system using a red LED for upstream transmission performance analysis with a BER analyzer.

In this work, two separate SMF fiber links via bidirectional power splitter are utilized for isolating the upstream and downstream frequencies in the remote nodes (RNs) as it reduces the Rayleigh backscattering (RB) noise interference in the proposed TWDM-PON system utilizing OFDM modulation [43, 47]. Table 2 presents the fiber and free-space link parameters used in this proposed work.

3 Results and Discussion

This section illustrates the information transmission performance investigation of the full-duplex TWDM-PON employing 4-QAM OFDM modulation with the VLC system on the basics of quality factor, BER, received optical power, EVM(%), constellation diagrams and eye diagrams. The performance of the proposed system at -6 dBm input power is analyzed for both downstream and upstream OFDM channels at 187.7 THz and 195.5 THz frequencies respectively over 10–140 m FSO link range, 10–100 km fiber link range and 2.5–200 Gbps data rate.

Figure 5 illustrates each stage output of the TWDM-OFDM PON with the VLC system for the free space and fiber link ranges of 10 m and 100 km respectively at 2.5 Gbps

Table 1 Switching Time of the proposed TWDM-OFDM PON with VLC system for upstream transmission

Timeslot	T_{s1} (s)	T_{s2} (s)
0	0	0.40×10^{-06}
1	0.40×10^{-06}	0.81×10^{-06}
2	0.81×10^{-06}	1.22×10^{-06}
3	1.22×10^{-06}	1.63×10^{-06}
4	1.63×10^{-06}	2.04×10^{-06}
5	2.04×10^{-06}	2.45×10^{-06}
6	2.45×10^{-06}	2.86×10^{-06}
7	2.86×10^{-06}	3.27×10^{-06}

Table 2 Fiber and free space link parameters used in the proposed system

S. no	Component name	Component parameters	Parameter value	Unit
1	SMF	Reference frequency	193.4	THz
		Length	10–100	km
		Attenuation	0.2	dB/km
		Dispersion	16.75	ps/nm/km
		Dispersion slope	0.075	ps/nm^2/k
		Effective area	80	μm^2
		Nonlinear index of refraction	26×10^{-21}	m^2/W
		Temperature	300	K
2	FSO	Range	10–140	m
		Transmitting aperture diameter	5	cm
		Receiver aperture diameter	10	cm
		Beam divergence angle	1108	mrad

data rate for a downstream OFDM (187.7 THz) channel. Figure 5a presents the transmitted bit sequence using PRBS and it is changed into a 4-QAM format utilizing QAM generator together with M-ary conversion and the subsequent constellation diagram of this sequence is illustrated in Fig. 5b. This 4-QAM modulated I and Q signals are modulated with 512 subcarriers to generate OFDM signals. After the LP cosine filter, Fig. 5c, d indicate the OFDM outputs of I and Q channels respectively. For transmission of the signal, it is modulated by OFDM and two pairs of MZM modulators at a center frequency of CW laser (187.7 THz) with either side of subcarrier bands as shown in Fig. 5e. Figure 5f, g depict the emission spectra of four 4-QAM OFDM modulation signals before and after fiber respectively. The generated spectrum is affected by fiber dispersion, attenuation and non-linearities before it reaches the two pairs of PIN photodetectors. This transmitted signal is noticed with the aid of PIN photodetector and the extracted OFDM subcarriers (I and Q) are presented in Fig. 5h, i respectively. After coherent demodulation of the subcarriers by OFDM demodulator, the received sequence is generated and it is proved with a constellation diagram at receiving end before DSP unit as depicted in Fig. 5j. With the DSP unit, Fig. 5k–m show the constellation diagrams after Bessel filter, resampling, and dispersion along with nonlinear compensation respectively. Also, Fig. 5n–p illustrate the constellation diagrams after the adaptive equalizer FOE and CPE respectively. After the DSP block and a QAM sequence decoder, the electrical spectrum of the resultant signal is shown in Fig. 5q. Finally, Fig. 5r, s show the optical spectra after a red LED and free-space link. The received signal is observed by a PIN photodetector and the resultant signal is analyzed in terms of eye diagram in BER analyser as shown in Fig. 5t.

Figure 6 presents the Q-factor performance of downstream and upstream received signals for 187.7 THz and 195.5 THz OFDM channels each at the transmission of 2.5 Gbps information in terms of increasing FSO link range (10–140 m) at a fixed fiber link range of 10 km. The dotted line presents the forward error correction (FEC) limit for the successful reception of the signal to accomplish the minimum 3.8×10^{-3} BER with 7% FEC overhead.

The quality factor is the in-build figure of merit (FOM) that determines the optical signal quality in terms of the SNR. For preferable system performance, a higher value of a quality factor is desired which provides a lower BER probability. Hence, an increment in Q-factor gives a decrement in BER and better network performance [50].

From the results reported in Fig. 6, it can be observed that as the free space transmission range increases, the received signal performance deteriorates in terms of transmission quality factor for both downstream and upstream channels. Also, the observed results show a better performance of the upstream channel (195.5 THz) than the downstream channel (187.7 THz). This is because the upstream channel has more multipath fading resilience in comparison to the downstream channel. The Q-factor for the downstream channel is measured as 26.00, 8.24, and 2.70 whereas for the upstream channel is measured as 26.88, 10.42, and 2.92 at 10 m, 70 m, and 140 m free space link range respectively. The results demonstrate a faithful transmission of 2.5 Gbps data over a free-space link range of 140 m with acceptable Q-Factor (minimum BER of 3.8×10^{-3} under 7% FEC) for both downstream and upstream channels. Figure 6 also presents the eye diagrams of the proposed TWDM-PON system at four FSO ranges of 20 m, 50 m, 80 m and 110 m for the upstream channel. It shows the distortions in the eye diagrams (high eye closure) of the received signals increases with increasing link range.

Figure 7 illustrates the BER and free space link range in the form of received optical power for 20 Gbps bidirectional TWDM-OFDM PON with a VLC system at a fiber link range of 10 km. The results show that as the received optical power improves, the free space link range decreases and the BER performance of the proposed system enhances. This is because at higher received optical power and lower FSO link range, the decision for the received signal can be smoothly taken by the demodulator. The BER value of downstream channel is computed as 1.23×10^{-149}, 3.81×10^{-8} and 3.44×10^{-3} and upstream channel is computed as 9.49×10^{-160}, 1.42×10^{-8} and 2.44×10^{-3} at the received optical power of -7 dBm (at FSO range = 10 m), -25 dBm (at FSO range = 100 m) and -33 dBm (at FSO range = 140 m) respectively. Also, an upstream channel performs better than downstream channel up to 100 m FSO range and after 100 m both show almost the same performance. The observed results demonstrate a faithful data transmission with acceptable BER value (3.8×10^{-3} under 7% FEC) over the maximum bidirectional FSO link range of 140 m for the received power of -33 dBm or higher in the presence of fiber nonlinearities, chromatic dispersion, attenuation and noise.

Figure 8 presents the EVM (%) versus fiber length at -6 dBm input power at 2.5 Gbps data rate per channel and 10 m free space link range. EVM is generally illustrated in percentage (%) to compute the received signal quality under the effect of distortion in fiber and is determined either from the decision component or the constellation diagram. The threshold boundaries (x = 0; y = 0) based decision algorithm for 4-QAM modulation format achieves a soft decision on the received symbols as shown in Fig. 9. EVM(%) of the received signals is measured as follows [50]:

$$EVM(\%) = \sqrt{\frac{\overline{\left| S - S_d^2 \right|}}{\overline{\left| S_d \right|^2}}} \times 100\% \qquad (8)$$

where S and S_d means the symbol sequence and decision of S respectively, and $\overline{(\dots)}$ denotes the mean value.

From the results reported in Fig. 8, it can be noted that the EVM(%) raises with the increase in fiber link range occurring in the inflated error level during data transmission. EVM(%) without DSP unit for the downstream signal is measured as 5.20, 61.18.40, and 87.62 whereas for the upstream signal is measured as 5.19, 58.97, and 87.37 at a fiber

Fig. 5 Proposed TWDM-PON using OFDM with VLC system outputs at each downstream transmission ▶
stage **a** transmitted bit sequence at 2.5 Gbps, **b** QAM constellation at transmitter, OFDM output after the
LP cosine filter for **c** I channel, **d** Q channel, **e** OFDM modulation output at transmitter (187.7 THz), emission spectra of four 4-QAM OFDM modulation outputs **f** before 100 km fiber link at transmitter, **g** after
100 km fiber link at receiver, **h** photo detector and OFDM demodulated output for I channel, **i** photo detector and OFDM demodulated output for Q channel, **j** received QAM constellation diagram at receiving end
before DSP, constellation diagrams after **k** Bessel filter, **l** resampling, **m** dispersion as well as nonlinear
compensation, **n** adaptive equalizer, **o** FOE and **p** CPE at receiving end after DSP, **q** electrical spectrum
of received signal after QAM sequence decoder, **r** optical spectrum after red LED **s** optical spectrum after
10 m FSO link, **t** eye diagram in BER analyser

link range of 10 km, 50 km, and 100 km respectively. Again, EVM(%) with DSP unit for
the downstream signal is measured as 14.83, 16.05, and 26.49 whereas for the upstream
signal is measured as 14.69, 15.87, and 24.68 at a fiber link range of 10 km, 50 km, and
100 km respectively. It is seen that initially almost up to 15 km fiber link range, EVM(%)
for both downstream and upstream channels with no DSP unit is almost 10% lower than
the channels with DSP unit. After that, EVM(%) for both channels with no DSP unit is
increased by almost 63% as compared to DSP unit channels at 100 km according to the
given EVM(%) Eq. (8). Further, the EVM limit of 17.5% for 4-QAM, as defined in 3GPP
specifications [51], is shown by the dotted line. Thus, it is observed that a faithful fiber
range of 10–60 km is obtained by using the DSP unit in the system. EVM is influenced by
a large range of issues like in-phase/quadrature-phase mismatches in the modulator/demodulator components because of dc offset, gain as well as phase differences. Moreover, phase
noise and frequency offset also lead to a constellation diagram with misplaced points causing worse modulation quality and more errors [50].

Figure 10 presents the Q-factor versus data rate for bidirectional channels of the proposed system over 10 km fiber link and 10 m FSO link range. It is observed that Q-factor
decreases with the increase in data rate because of the detrimental effects of fiber nonlinearity at the information rate of the system. Also, it can be seen that the upstream channel shows better performance as compared to the downstream channel. As shown, for the
downstream channel the Q-factor is measured as 25.41, 9.80, and 1.41 and for the upstream
channel the Q-factor is measured as 25.44, 10.00, and 2.23 at the transmission rate of
10 Gbps, 100 Gbps and 200 Gbps respectively. The results demonstrated a successful data
transmission rate with acceptable Q factor (under 7% FEC) from 20 to 190 Gbps for downstream channel and 20–200 Gbps for the upstream channel. Figure 10 also illustrates the
constellation diagrams of the proposed system at different transmission rates in the proposed system. These constellation diagrams interpreted that received signal distortion deteriorates at a lower transmission rate and the signal can be successfully regenerated at the
receiver.

Further, the comparative performance of the proposed TWDM-PON system with the
latest previous literature works as presented in Table 3 illustrates that the proposed system
reports superior performance in the form of maximum free space link range, fiber length
and data rate. The higher information rate over long-distance wired-wireless link per channel than previous work is attained by using 4-QAM OFDM modulation format, a red LED
enabled VLC system and DSP unit for enhanced performance of the fiber-wireless link.
While the previously reported works in the literature utilize modulation formats like POL-
MUX, VLLC system and no DSP unit capable of transmitting only up to maximum 10 m
free space and 50 km fiber link range at 10 Gbps information with no DSP unit. Thus the
proposed system has advantages of high data rate, high bandwidth, support a large number
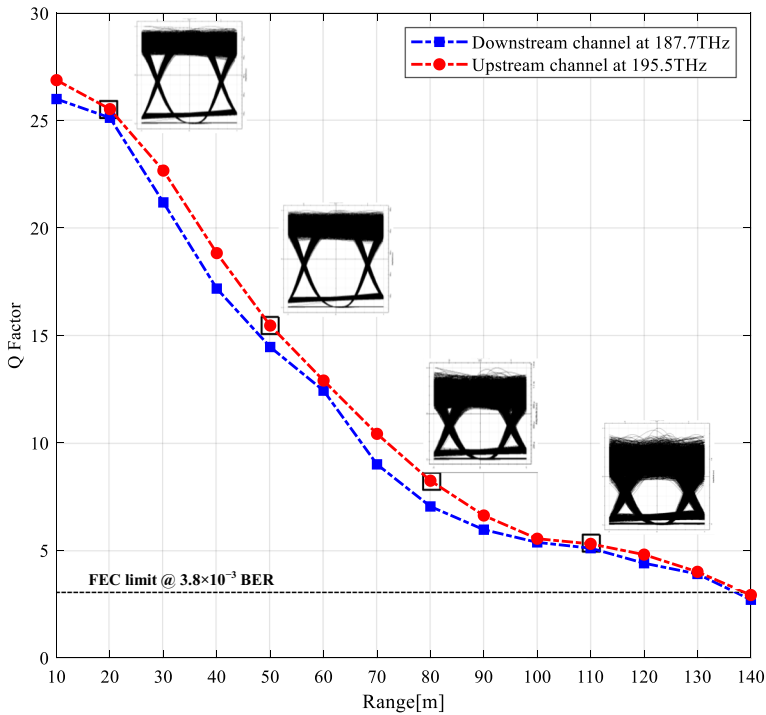of consumers, cost-effectiveness, reliability, scalability, easy upgradeability.

(a)

(b)

(c)

(d)

(e)

(f)

(g)

(h)

(i)

(j)

(k)

(l)

(m)

(n)

(o)

(p)

(q)

(r)

(s)

(t)
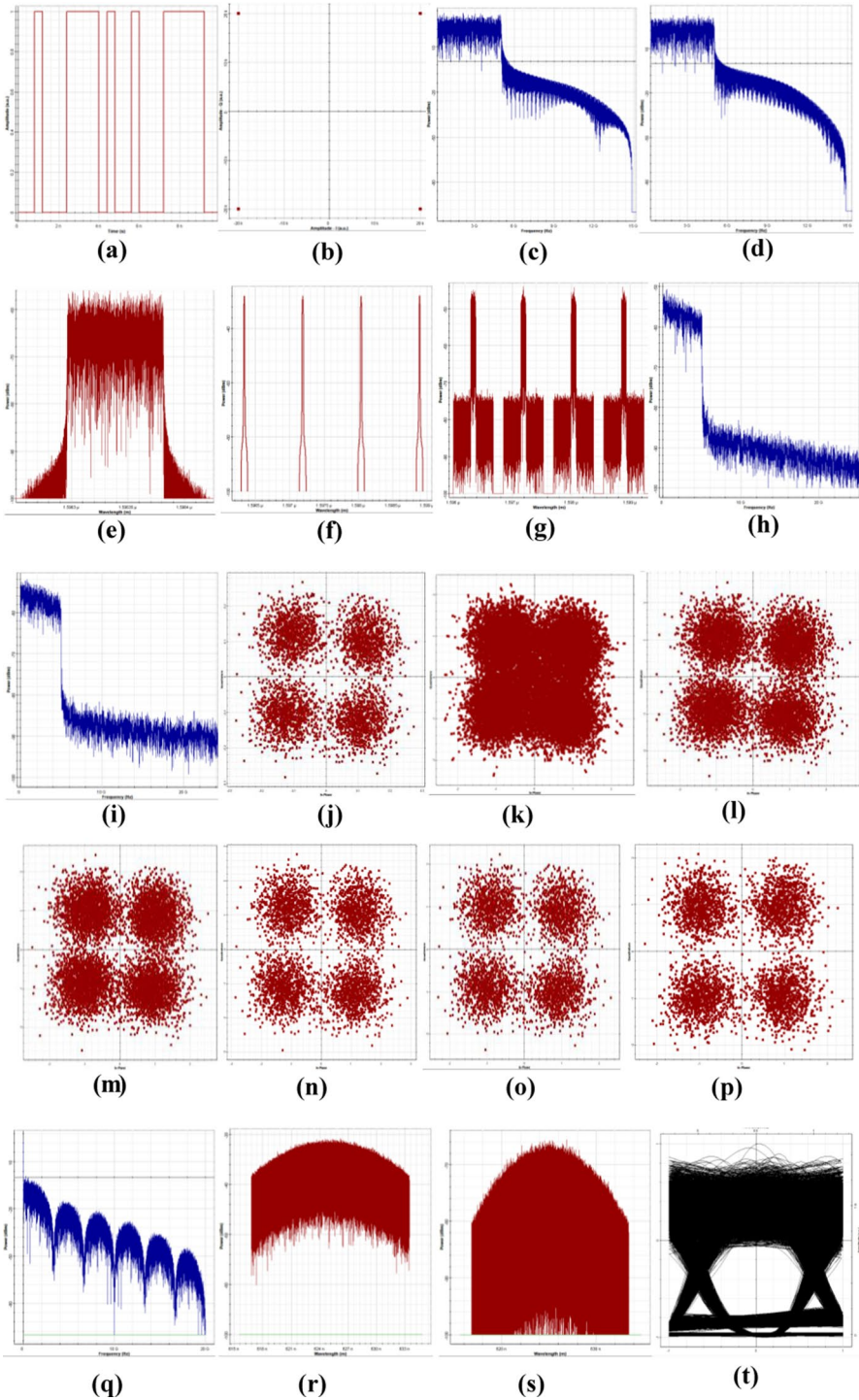
Fig. 6 Q-Factor versus free space link range for downstream and upstream channels. Insets: eye diagrams of the upstream channel at the different range

4 Conclusion

In this paper, a next-generation NG-PON2 based symmetric and full-duplex 4×200 Gbps TWDM-PON using 4-QAM OFDM modulation format with red LED enabled VLC system has been designed and demonstrated for long-reach and high-speed applications. From the results, it is concluded that the maximum acceptable free space and fiber range for the proposed system varies from 10 to 140 m at a fixed fiber link of 10 km and 10 km to 60 km at a fixed free-space link of 10 m respectively under the BER of 3.8×10^{-3} at 20 Gbps transmission rate. The impact of increasing the proposed link range on the proposed system demonstrates that the received optical power of the signal is decreased as the free space link increases. Also, it is investigated that EVM decreases by almost 52% with the use of the DSP unit in the proposed system
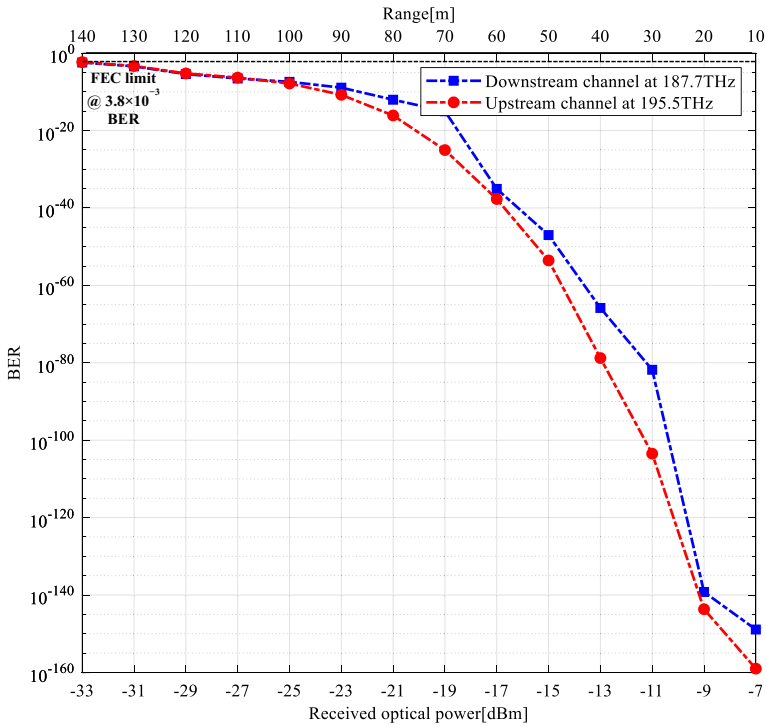
Fig. 7 BER and range versus received optical power for upstream and downstream channels

causing proposed link enhancement as compared to the system without a DSP unit. The maximum transmission rate for the designed system with free space and fiber link range of 10 m and 10 km respectively is 200 Gbps. The achieved results reveal the better performance of upstream signals than downstream signals and provide clear constellation diagrams. Further, the proposed system performance is correlated with the recent previous literature indicating the proposed link works significantly superior in terms of maximum transmission distance and information rate. Thence, the TWDM-PON using 4-QAM OFDM modulation with a red LED VLC system can enhance the utilization of fiber-VLC links and achieve a smooth up-gradation to next-generation access networks requiring 1 Tbps. This system can be used to provide cost-effective, high-speed and long wired-wireless link range services from rural areas to urban areas.
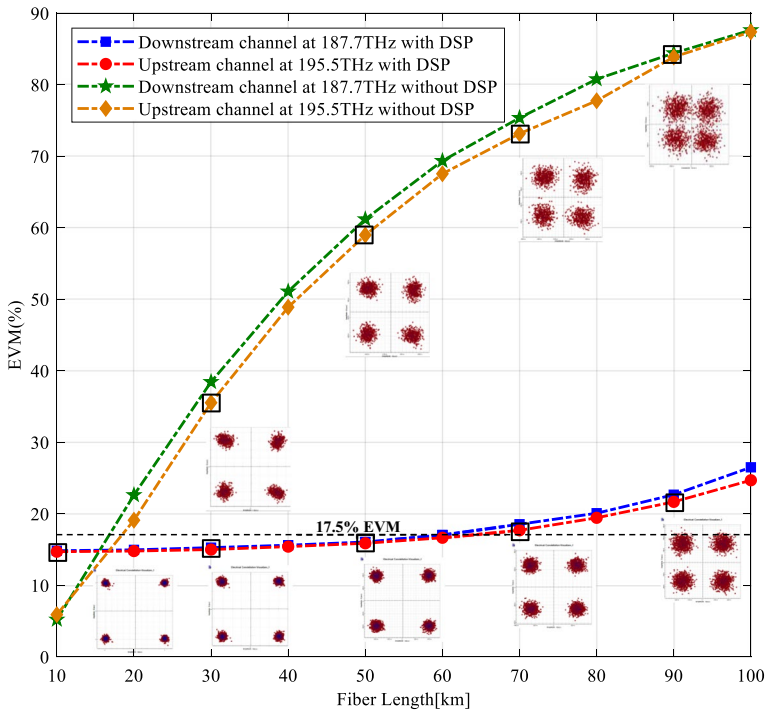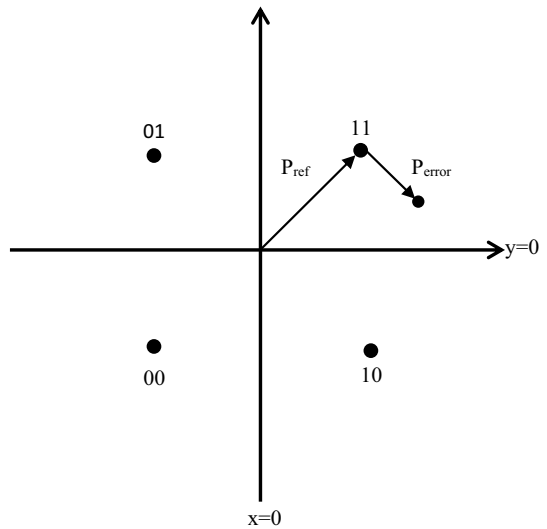
Fig. 8 EVM (%) versus fiber length of both downstream and upstream channels with and without DSP unit. Insets: constellation diagrams of upstream channels with and without DSP unit at different fiber length
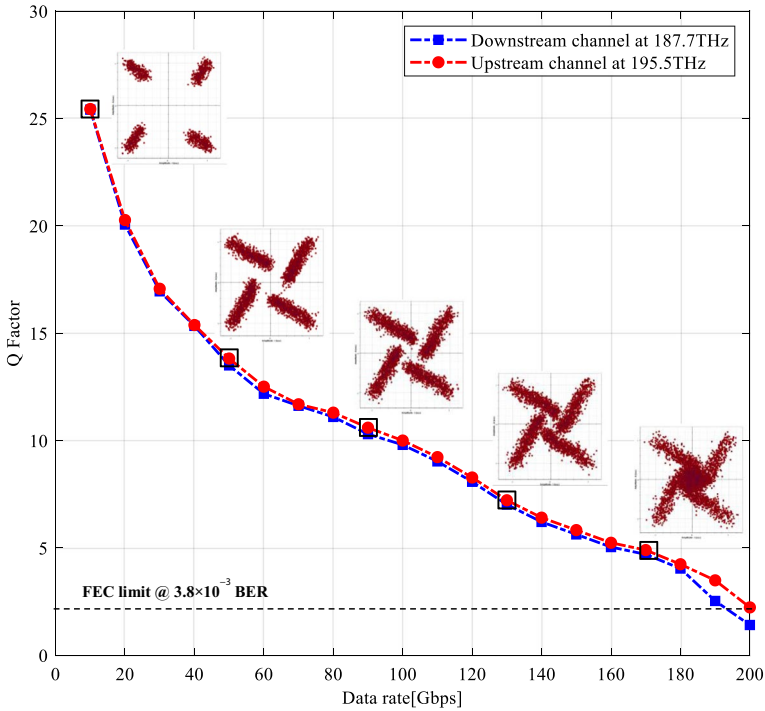

Fig. 9 Error vector magnitude computation

Fig. 10 Q-factor versus bit rate of downstream and upstream channels. Insets: constellation diagrams of upstream channels at different data rates

Table 3 Comparative performance of the proposed TWDM-PON system with previous works

Reference	Technique	Maximum free space range (m)	Maximum SMF length (km)	Maximum data rate (Gbps)	DSP unit
[39]	Integrated WDM–CAP–PON with blue LD based VLLC system	4.5	20	10	No
[41]	FDM/OQAM based WDM fiber/ blue LD based VLLC system	4.5	50	3.2	No
[40]	OFDM for fiber/ blue LD based VLLC system	8	20	2.5	No
[50]	Hybrid fiber-wired/fiber-LD wireless/fiber-VLC/fiber-invisible light communication (IVLC)	10	50	2.5	No
[52]	OFDM based LD wireless system employing polarization multiplexing technique (POLMUX)	10	50	10	No
Proposed work	TWDM-PON with OFDM using a red LED VLC system	140	60	200	Yes

Declarations

Conflict of interest The authors declare that they have no conflict of interest.

References

1. Han, J., Zhang, J., Zhao, Y., & Gu, W. (2013). Channel capacity and space-time block coding for coherent optical MIMO multi-mode fiber links. *Optik, 124*(10), 922–927.
2. Ren, F., Li, J., Hu, T., Tang, R., Yu, J., Mo, Q., He, Y., Chen, Z., & Li, Z. (2015). Cascaded mode-division-multiplexing and time-division-multiplexing passive optical network based on low mode-crosstalk FMF and mode MUX/DEMUX. *IEEE Photonics Journal, 7*(5), 1–9.
3. Odeyemi, K. O., & Owolawi, P. A. (2020). Wireless energy harvesting based asymmetric RF/FSO system with transmit antenna selection and receive diversity over M-distribution channel and non-zero boresight pointing error. *Optics Communications, 461,* 125219.
4. Hu, T., Li, J., Ren, F., Tang, R., Yu, J., Mo, Q., Ke, Y., Du, C., Liu, Z., He, Y., et al. (2016). Demonstration of bidirectional PON based on mode division multiplexing. *IEEE Photonics Technology Letters, 28*(11), 1201–1204.
5. Valcarenghi, L., Van, D. P., Raponi, P. G., Castoldi, P., Campelo, D. R., Wong, S. W., Yen, S. H., Kazovsky, L. G., & Yamashita, S. (2012). Energy efficiency in passive optical networks: Where, when, and how? *IEEE Network, 26*(6), 61–68.
6. Radivojević, M., & Matavulj, P. (2019). Techno-economic analysis of multiservice EPON deployment. *Transactions on Emerging Telecommunications Technologies, 30*(6), 1–18. https://doi.org/10.1002/ett.3613
7. Yeh, C. H., Chow, C. W., Chen, H. Y., & Liu, Y. L. (2014). 115 Gbit/s downstream and 10 Gbit/s upstream TWDM-PON together with 11.25 Gbit/s wireless signal utilizing OFDM-QAM modulation. *Optical Fiber Technology, 20*(2), 84–89.
8. Lin, B., Li, Y., Zhang, S., & Tang, X. (2015). Asymmetrical TWDM-PON with 4 × 25-Gb/s downstream DSB OFDM and 4 × 10-Gb/s upstream OOK modulations. *Optical Fiber Technology, 26,* 206–210.
9. Šprem, M., & Babić, D. (2019). Wavelength reuse WDM-PON using RSOA and modulation averaging. *Optics Communications, 451,* 1–5.
10. Tang, X., Zhou, J., Guo, M., Qi, J., Hu, F., Qiao, Y., & Lu, Y. (2018). 40-Gb/s PAM4 with low-complexity equalizers for next-generation PON systems. *Optical Fiber Technology, 40,* 108–113.
11. Zhang, W. F., Xin, X. J., Zhang, Q., Zhang, Z. X., Nai, W., & Shi, Y. (2010). Centralized light-wave WDM-PON employing DQPSK downstream and OOK remodulated upstream signals. *Journal of China Universities of Posts and Telecommunications, 17*(4), 125–128.
12. Shao, Y., Chen, F., Wang, A., Luo, Y., & Chen, L. (2017). Application research on 4-pulsed amplitude modulation in 10 Gb/s passive optical access systems. *Optik, 146,* 63–68.
13. Gill, H. K., Walia, G. K., & Grewal, N. S. (2019). Performance analysis of mode division multiplexing IS-OWC system using Manchester, DPSK and DQPSK modulation techniques. *Optik, 177,* 93–101.
14. Selvendran, S., Sivanantha Raja, A., Esakki Muthu, K., & Lakshmi, A. (2019). Certain investigation on visible light communication with OFDM modulated white LED using optisystem simulation. *Wireless Personal Communications, 109,* 1377–1394.
15. Kaur, A., Kaur, B., & Singh, K. (2017). Design and performance analysis of bidirectional TWDM-PON employing QAM-OFDM for downstream and re-modulation for upstream. *Optik, 134,* 287–294.
16. Lyu, W. C., Wang, A., Xie, D., Zhu, L., Guan, X., Wang, J., & Xu, J. (2018). Self-homodyne optical OFDM for broadband WDM-PONs with crosstalk-free remodulation and enhanced tolerance to Rayleigh noise. *Optics Communications, 414,* 77–82.

17. Grover, A., & Sheetal, A. (2020). A cost-effective high-capacity OFDM based RoFSO transmission link incorporating hybrid SS-WDM-MDM of Hermite Gaussian modes. *Optoelectronics and Advanced Materials—Rapid Communications, 14*(3–4), 136–145.

18. Grover, A., Sheetal, A., & Dhasarathan, V. (2020). Performance analysis of mode division multiplexing based free space optics system incorporating on–off keying and polarization shift keying under dynamic environmental conditions. *Wireless Networks, 26,* 3439–3449.

19. Zhang, J., Li, F., Li, J., & Li, Z. (2017). 95.16-Gb/s mode-division-multiplexing signal transmission in free-space enabled by effective-conversion of vector beams. *IEEE Photonics Journal, 9*(4), 1–9.

20. Kachhatiya, V., & Prince, S. (2016). Four-fold increase in users of time-wavelength division multiplexing (TWDM) passive optical network (PON) by delayed optical amplitude modulation (AM) upstream. *Optical Fiber Technology, 32,* 71–81.

21. Kachhatiya, V., & Prince, S. (2018). Downstream performance analysis and optimization of the next generation passive optical network stage 2 (NG-PON2). *Optics and Laser Technology, 104,* 90–102.

22. Savojbolaghchi, H., Sadough, S. M. S., Dabiri, M. T., & Ansari, I. S. (2019). Generalized channel estimation and data detection for MIMO multiplexing FSO parallel channels over limited space. *Optics Communications, 452,* 158–168.

23. Anis, M. I., Qureshi, M. S., & Zafar, S. (2017). Demonstration of TWDM-PON backward compatibility with conventional GPON. *Wireless Personal Communications, 95,* 581–592.

24. Yeh, C. H., Chow, C. W., Gu, C. S., Guo, B. S., Cheng, Y. J., & Chen, J. H. (2018). Performance analysis of free space optical communication traffic integrated with passive optical network. *Electronics Letters, 54*(21), 1228–1229.

25. Singh, M., Malhotra, J., Mani Rajan, M. S., Dhasarathan, V., & Aly, M. H. (2020). Performance evaluation of 6.4 Tbps dual polarization quadrature phase shift keying Nyquist-WDM superchannel FSO transmission link: Impact of different weather conditions. *Alexandria Engineering Journal, 59*(2), 977–986.

26. Moghaddasi, M., Mamdoohi, G., Muhammad Noor, A. S., Mahdi, M. A., & Ahmad Anas, S. B. (2015). Development of SAC-OCDMA in FSO with multi-wavelength laser source. *Optics Communications, 356,* 282–289.

27. Mallick, K., Mandal, P., Mukherjee, R., Mandal, G. C., Das, B., & Patra, A. S. (2020). Generation of 40 GHz/80 GHz OFDM based MMW source and the OFDM-FSO transport system based on special fine tracking technology. *Optical Fiber Technology, 54,* 102130.

28. Prabu, K., Charanya, S., Jain, M., & Guha, D. (2017). BER analysis of SS-WDM based FSO system for Vellore weather conditions. *Optics Communications, 403,* 73–80.

29. Mohd Nor, N. A., Ghassemlooy, Z., Zvanovec, S., Khalighi, M. A., Bhatnagar, M. R., Bohata, J., & Komanec, M. (2019). Experimental analysis of a triple-hop relay-assisted FSO system with turbulence. *Optical Switching and Networking, 33,* 194–198.

30. Chen, M., Lu, H., Chen, D., Jin, J., & Wang, J. (2020). An efficient MIMO–OFDM VLC system of combining space time block coding with orthogonal circulant matrix transform precoding. *Optics Communications, 473,* 125993.

31. Li, H., Zhang, Y., Chen, X., Wu, C., Guo, J., Gao, Z., Pei, W., & Chen, H. (2015). 682 Mbit/s phosphorescent white LED visible light communications utilizing analog equalized 16QAM-OFDM modulation without blue filter. *Optics Communications, 354,* 107–111.

32. Ma, J., He, J., Chen, Q., Shi, J., Zhou, Z., Cheng, Y., & Xiao, Y. (2018). A MB-CAZAC precoding combined with 128/64/32/16-QAM modulation for OFDM-VLC system. *Optics Communications, 424,* 154–158.

33. Lu, M., Xiao, S., Zhang, L., Zheng, L., Fang, J., Huang, T., & Hu, W. (2019). Real-time VLC system integrated with positioning beacon transmission based on 2ASK-CE-OFDM coding. *Optics Communications, 452,* 252–257.

34. Deng, R., He, J., Chen, M., & Zhou, Y. (2018). Experimental demonstration of a real-time gigabit OFDM-VLC system with a cost-efficient precoding scheme. *Optics Communications, 423,* 69–73.

35. Chow, C. W., Yeh, C. H., Liu, Y. F., Huang, P. Y., & Liu, Y. (2013). Adaptive scheme for maintaining the performance of the in-home white-LED visible light wireless communications using OFDM. *Optics Communications, 292,* 49–52.

36. Zhang, J., Hong, X., Liu, J., & Guo, C. (2018). Experimental demonstration of an OFDM based visible light communication system using inter-block precoding and superimposed pilots. *Optics Communications, 412,* 219–225.

37. Li, X., Min, C., Gao, S., Wang, Y., Chen, X., & Chen, H. (2019). Experimental demonstration of a real-time multi-channel uplink VLC system. *Optics Communications, 453,* 124420.

38. Chi, N., & Shi, J. (2015). Investigation on overlapping interference on VLC networks consisting of multiple LEDs. *ICT Express, 1,* 63–66.

39. He, J., Dong, H., Deng, R., Shi, J., & Chen, L. (2016). WDM-CAP-PON integration with VLLC system based on optical frequency comb. *Optics Communications, 374,* 127–132.

40. Wei, Y., He, J., Deng, R., Shi, J., Chen, S., & Chen, L. (2017). An approach enabling adaptive FEC for OFDM in fiber-VLLC system. *Optics Communications, 405,* 329–333.

41. Shi, J., He, J., Zhang, R., Deng, R., & Xiao, Y. (2018). OFDM/OQAM based WDM fiber VLLC system employing improved channel estimation method. *Optics Communications, 427,* 578–583.

42. Chen, C., Zhong, W. D., & Wu, D. (2016). Integration of variable-rate OWC with OFDM-PON for hybrid optical access based on adaptive envelope modulation. *Optics Communications, 381,* 10–17.

43. Lu, I. C., Yeh, C. H., Hsu, D. Z., & Chow, C. W. (2016). Utilization of 1-GHz VCSEL for 11.1-Gbps OFDM VLC wireless communication. *IEEE Photonics Journal, 8*(3), 1–6.

44. Matheus, L., Pires, L., Vieira, A., Vieira, L. F. M., Vieira, M. A. M., & Nacif, J. A. (2019). The internet of light: Impact of colors in LED-to-LED visible light communication systems. *Internet Technology Letters, 2*(1), 1–6.

45. Kaur, A., Sheetal, A., & Miglani, R. (2017). Impact of optical modulation formats on 10 G/2.5 G asymmetric XG-PON system. *Optik, 149,* 351–358.

46. Yang, H., Li, J., Lin, B., Wan, Y., Guo, Y., Zhu, L., Li, L., He, Y., & Chen, Z. (2013). DSP-based evolution from conventional TDM-PON to TDM-OFDM-PON. *Journal of Lightwave Technology, 31*(16), 3035–3041.

47. Li, C., Hu, R., Li, H. B., Luo, M., Yang, Q., & Yu, S. (2017). Digital OFDM-PON based on delta-sigma modulation employing binary IM-DD channels. *IEEE Photonics Journal, 9*(2), 1–7.

48. Kaur, A., Singh, M. L., & Sheetal, A. (2014). Simulative analysis of co-existing 2.5 G/10 G asymmetric XG-PON system using RZ and NRZ data formats. *Optik, 125*(14), 3637–3640.

49. Kumari, M., Sharma, R., & Sheetal, A. (2019). Comparative analysis of high speed 20/20 Gbps for long-reach NG-PON2. *Journal of Optical Communications, 66,* 1–14.

50. Sheetal, A., & Singh, H. (2018). 5 × 10 Gbps WDM-CAP-PON based on frequency comb using OFDM with blue LD. *Optical and Quantum Electronics, 50,* 1–14.

51. Nguyen, D.-N., Bohata, J., Spacil, J., Dousek, D., Komanec, M., Zvanovec, S., Ghassemlooy, Z., & Ortega, B. (2019). M-QAM transmission over hybrid microwave photonic links at the K-band. *Optics Express, 27*(23), 33745.

52. Mallick, K., Mukherjee, R., Das, B., Mandal, G. C., & Patra, A. S. (2018). Bidirectional hybrid OFDM based Wireless-over-fiber transport system using reflective semiconductor amplifier and polarization multiplexing technique. *AEU—International Journal of Electronics and Communications, 96,* 260–266.

Meet Kumari was born in Gurdaspur, Punjab, India on 9th, September 1990. The author received her M.Tech. degree in Electronics and Communication Engineering from Guru Nanak Dev University, Regional Campus Jalandhar, Punjab, India in 2015 and received her B.Tech. degree in Electronics and Communication Engineering from Guru Nanak Dev University, Regional Campus Gurdaspur, Punjab, India in 2015. Currently, she is working as an Assistant Professor in Chandigarh University, Mohali, Punjab, India. The author is a Reviewer of many Reputed International Journals. His area of interest includes optical communication, green communication, next generation networks and wireless sensor networks.

Dr. Anu Sheetal was born in Bahadurgarh, Haryana, India, on 18th September, 1972. She obtained her Bachelor's degree in Electronics Engineering with distinction from the Department of Electronics and Communication Engineering, Punjabi University, Patiala, India in 1994 and Master's degree in Electronics Engineering from Punjab Technical University, Jalandhar, India in 2003. She obtained his Ph.D. degree from Punjab Technical University, Jalandhar, in 2012. She worked as a Design Engineer at Gilard Electronics Private Limited, Mohali, from 1994 to 1997. She then joined AIET, Faridkot as a lecturer and became Head of Department in 1999. In 2004, she joined Guru Nanak Dev University, Regional campus, Gurdaspur, Punjab, India in the Department of Electronics and Communication Engineering as a lecturer and became Assistant Professor in the Department of Electronics and Communication Engineering. Presently, she is working as Sr. Assistant Professor and Head of the department in the same institute. Her present interests are Optical Communication Systems, soliton transmission and DWDM Networks, WDM-PON, RoF etc. She has over 50 research papers published/presented in International/National Journals/Conferences to her credit. She is a life member of The Institution of Electronics and Telecommunication Engineers (IETE), New Delhi (India), Indian Society of Technical Education (ISTE), Optical Society of India, Kolkata (OSI), International Association of Engineers (IAENG). She is acting as a member of editorial board of The International Journal of VLSI and Signal Processing Applications (IJVSPA), International Journal of Research IJRICE, ISP Journal of Electronics Engineering. She is acting as technical reviewer for many international journals such as Journal of SPIE—Optical Engineering, OPTIK etc.

Dr. Reecha Sharma obtained her Bachelor's degree in Electronics and Instrumentation Engineering from MMEC Mullana, Haryana, India in 2003 and Master's degree in Electronics Instrumentation and control Engineering form T.I.E.T., Patiala, Punjab, India 2005. She obtained his Ph.D. degree from Punjabi University, Patiala, in 2016. Presently, she is working as Assistant Professor in Punjabi University, Patiala. Her present interests are digital image processing, digital signal processing, feature extraction, face recognition, filter designing, opto-imaging, control engineering, fuzzy logics, artificial neural networks and optimization techniques. She has over 178 research papers published/presented in International/National Journals/Conferences to her credit. The author is a Reviewer of many Reputed International Journals.